Bremsstrahlung Cross Section of 60-Mev Electrons in Lead*

C. D. CURTIS†
University of Illinois, Urbana, Illinois
(Received May 12, 1952)

Sixty-Mev electrons from a pulsed betatron passed through lead foils of thicknesses 0.001, 0.005, and 0.015 inch placed in a magnetic cloud chamber. Measurements of approximately 1100 large energy losses gave the differential bremsstrahlung cross section as a function of x-ray energy for the high energy portion of the x-ray spectrum. Corrections were applied for instrumental discrimination and for multiple radiation and ionization energy losses in the foils. While the shape of the top 30 percent of the x-ray spectrum agreed with the theory within experimental uncertainty, the magnitude of the cross section was about 7 percent lower than theory.

INTRODUCTION

IN 1934 Bethe and Heitler[1,2] developed a theory for bremsstrahlung production by relativistic electrons. They made calculations using as targets a bare nucleus and a nucleus screened by the electrons of the Thomas-Fermi atom. Use of the Born approximation required that $Ze^2/\hbar v \ll 1$ before and after collision of the electron with the nucleus, where v is the electron speed. Even when the speeds approach that of light, however, $Ze^2/\hbar v$ becomes approximately 0.6 for lead. In this case Parzen[3] has pointed out that any error in the cross section integrated over all angles of the emergent electron and quantum should be no greater than $(\mu/E_0)^{\frac{1}{2}}$, where μ and E_0 are, respectively, the rest and total energy of the incident electron. Schiff[4–6] obtained an analytic expression for a differential energy spectrum for a thin target. In the worst case of large Z and partial screening this was no more than 4 percent higher than the numerical calculations of Bethe and Heitler.

Measurements[7–14] of the total radiation energy loss by electrons of various energies from a few tenths to 13.5 Mev have yielded rather inconsistent results, from approximately 15 percent lower to at least 40 percent higher than those predicted by the Bethe-Heitler theory. One of the difficulties in the measurement of energy loss of electrons passing through foils has been that of interpretation because of multiple scattering within the foils.[12]

Measurements[15,16] of the energy loss of cosmic-ray electrons with energies up to 200 Mev passing through lead plates in a cloud chamber have confirmed the theory within an uncertainty of approximately 20 percent.

Lanzl[17] found the total radiation cross section of 17.6-Mev electrons in high Z elements to be 10 percent lower than theory with an uncertainty of about 10 percent.

The experimental shape of the x-ray energy spectrum from monokinetic electrons is in general agreement with theory at energies of 20 and 300 Mev.[18–20]

The present paper describes a measurement of the differential bremsstrahlung cross section for 60-Mev electrons in lead. When the electrons passed through lead foils in a magnetic cloud chamber, the energies for the x-ray quanta which were emitted were determined for the top 30 percent of the x-ray spectrum. The difference observed between the incident and emergent energies of an electron thus gave approximately the quantum energy $h\nu = E_0 - E$.

EXPERIMENTAL ARRANGEMENT

A. Source of Electrons

Electrons were accelerated to an energy of 82.5 Mev in a pulsed betatron.[21] No special device was used to extract the electron beam, although this would be desirable to obtain a monoenergetic beam with maximum intensity. For cloud-chamber operation, however, the electrons which normally emerged through the vacuum chamber wall after expansion of the electron orbit gave far more than sufficient intensity. Although the betatron operated at 82.5 Mev, the electrons escaping from the vacuum chamber were greatly degraded by scattering from the injector structure and by passing through the chamber wall. The mean energy of

* Assisted by the joint program of the ONR and AEC.
† Now at Argonne National Laboratory, Chicago, Illinois.
[1] H. Bethe and W. Heitler, Proc. Roy. Soc. (London) **146**, 83 (1934).
[2] H. Bethe, Proc. Cambridge Phil. Soc. **30**, 524 (1934).
[3] G. Parzen, Phys. Rev. **81**, 808 (1951).
[4] L. I. Schiff, Phys. Rev. **83**, 252 (1951).
[5] L. Katz, Can. J. Phys. **29**, 518 (1951).
[6] G. D. Adams, Phys. Rev. **74**, 1707 (1948).
[7] H. Klarman and W. Bothe, Z. Physik **101**, 489 (1936).
[8] J. J. Turin and H. R. Crane, Phys. Rev. **52**, 63 (1937).
[9] L. J. Laslet and D. G. Hurst, Phys. Rev. **52**, 1035 (1937).
[10] A. J. Ruhlig and H. R. Crane, Phys. Rev. **53**, 618 (1938).
[11] W. A. Fowler and J. Oppenheimer, Phys. Rev. **54**, 320 (1938).
[12] M. M. Slawsky and H. R. Crane, Phys. Rev. **56**, 1203 (1939).
[13] Ivanov, Walther, Sinelnikov, Taranov, and Abramovich, J. Phys. (U.S.S.R.) **4**, 319 (1941).
[14] Van Atta, Petrauskas, and Myers, Am. J. Roentgenol & Radium Therapy **50**, 803 (1943).
[15] P. M. S. Blackett, Proc. Roy. Soc. (London) **165**, 11 (1938).
[16] C. D. Anderson and S. H. Neddermeyer, Phys. Rev. **50**, 263 (1936).
[17] L. H. Lanzl and A. O. Hanson, Phys. Rev. **83**, 959 (1951).
[18] H. W. Koch and R. E. Carter, Phys. Rev. **77**, 165 (1950).
[19] Powell, Hartsough, and Hill, Phys. Rev. **81**, 213 (1951).
[20] J. W. Dewire and L. A. Beach, Phys. Rev. **83**, 476 (1951).
[21] Kerst, Adams, Koch, and Robinson, Rev. Sci. Instr. **21**, 462 (1950).

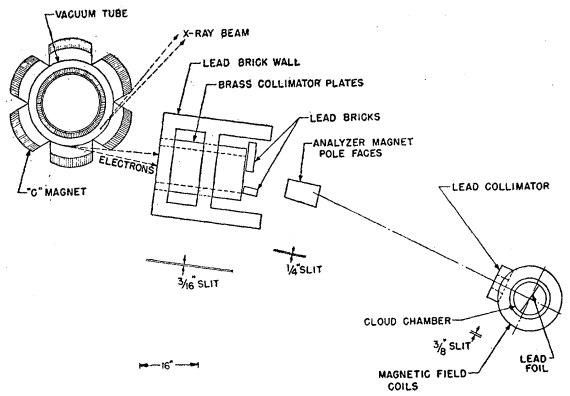

FIG. 1. Experimental layout.

the electrons entering the cloud chamber was approximately 60 Mev. Most of them had traveled a slanting path through the wall much longer than the wall thickness. Figure 1 is a diagram of the experimental arrangement. Parallel brass plates two ft long, which were imbedded in lead bricks, collimated electrons from the betatron into a sheet $\frac{3}{16}$ in. thick. The electrons then passed between the plates of a permanent magnet with a field strength of approximately 2500 gauss. The magnet effected some energy analysis of the electrons and separated them from any x-rays present. The remaining electrons with a limited energy spread entered a cloud chamber 8 in. in diameter through a $\frac{3}{8}$-in. lead collimator slit to produce tracks spread over a width of 4 in. in the chamber.

B. Detection of Radiation Straggling

For the high energy end of the x-ray spectrum, an especially thin target foil is desired to insure measurement of very low energy straggled electrons whose energies will permit an accurate energy determination of the x-rays emitted. This will be the case only if the target is thin enough to render multiple radiation losses negligible and ionization loss very small. Of particular concern is the energy loss experienced by the straggled electron through excessive multiple scattering after the large radiation loss has occurred. One is limited, however, in the minimum thickness practicable by the need for keeping the number of cloud-chamber photographs necessary for reasonable statistics from becoming prohibitive, particularly in terms of time required for analysis. A total of 20 400 pictures were taken, with and without lead foils of varying thicknesses. Of these, 1700 were taken at various times during the experiment with no foils in the cloud chamber. These pictures furnished data for calibration of the primary electron energies. Some 4900 pictures were taken with a foil thickness of 0.005 in. Five parallel foils were placed perpendicular to the path of the electrons to increase the chance of a radiation event for each picture. This arrangement permitted measurement of straggled electron energies up to a few Mev. However, with the available field strength, the spacing was too close for accurate measurement of more than about 10 Mev. For observation of higher energy straggled electrons and for greater ease of analysis, 11 200 pictures were taken using one foil 0.015 in. thick across the center of the cloud chamber. On these pictures, radii were measured up to 25 cm corresponding to a maximum energy of about 21 Mev. Corrections for energy loss by the straggled electrons in foils 0.015 and 0.005 in. thick were necessary. Still thinner foils of 0.001 in. were used to reduce further the necessary corrections. The radiation events occurred very infrequently in these foils, particularly quite near the high energy tip of the x-ray spectrum. Only 2600 pictures were taken with five such foils in the chamber; therefore, the statistics were very poor indeed. The data from these pictures serve only as a rough check on the results from the other foil arrangements.

The number of electron tracks passing through the foils varied from picture to picture, but from six to ten tracks for each provided a good distribution without bunching.

The cloud-chamber magnetic field was produced by current from a pulsed generator.[22] A timing circuit triggered the betatron at the peak of the current pulse which had a duration of about 350 milliseconds. The cloud chamber and betatron were operated once every 30 seconds. Because of a slow variation of the field current with time, it was regularly monitored.

The average value of the peak magnetic field strength was approximately 3100 gausses with the value at a specified time determined to within 2 percent. The calibration of the field current meter in terms of steady field strength was accomplished with a proton magnetic moment detector. The strength of the pulsed field was then determined from the relative values of the voltages induced in a rotating coil placed in the fluxes of the steady and pulsed fields. A second method of obtaining the pulsed field strength used a General Electric fluxmeter which integrated the time rate of change of magnetic flux.

The cloud chamber had an air filling to approximately 26 lb per sq in. absolute. The condensing vapor was an ethyl alcohol-water mixture of 3:1. Two General Electric FT-422 lamps illuminated a region $\frac{3}{4}$ in. deep in the chamber. They were singly pulsed for photography and multiply pulsed 60 times per second for visual observation.[22]

The cloud-chamber tracks were photographed stereoscopically by a single camera and two mirrors.[18] For best sensitivity and contrast most pictures were taken on Eastman Kodak linograph-ortho film which was processed in D-11 developer.

C. Analysis of Tracks

All pictures were scanned for events on plane projection tables which used lenses matched to the one in

[22] C. D. Curtis, Ph.D. thesis, University of Illinois (1951, unpublished).

the camera. Radii of tracks projected into the horizontal plane to original size were measured on these tables. For the radiation events, radii of the straggled electrons were included up to 25 cm on the one-foil pictures and up to 17 cm on the five-foil pictures, although the latter limit was reduced later in evaluation of the data. All tracks penetrating the foils were counted as traversals with the exception of a very few low energy tracks which could be detected as having less than a fixed minimum radius. This limit was 30 cm for the five-foil pictures and 45 cm for the one-foil pictures, corresponding to about 27.4 and 41.3 Mev, respectively. An occasional picture was discarded because of an excessive number or bunching of the tracks. A first glance could determine without discrimination the condition of the picture. Data were also collected on events such as secondary electrons and electron created pairs. A few large electron energy losses occurred in the cloud-chamber gas and one electron created pair was observed there. All pictures were scanned a second time for radiation events with special attention given to short chord length tracks. In the case of one-foil pictures, an attempt was made to miss none of the 25-cm radius straggled tracks with a chord length ≥ 3.5 cm. Later in the treatment of corrections to the data, a longer minimum chord length was used.

Another examination of the pictures was made by projection through the original camera-mirror system used for the photography. A stereo-projection table[18] provided flexibility for measuring all angles necessary to describe a track in three dimensions. The dip angles made by the incident and emergent tracks with the horizontal plane and the angles between their projections in this plane were measured. The dip angle was necessary for determining the electron energy, and the angular distributions were used in making corrections to the data.

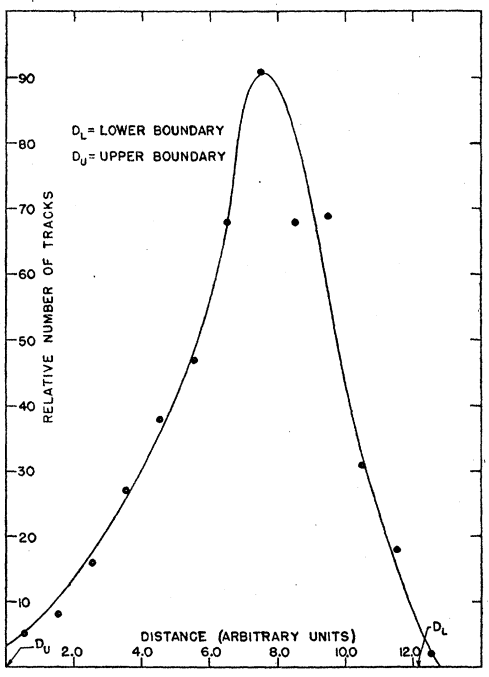

FIG. 2. Vertical position distribution of tracks at the 15-mil foil.

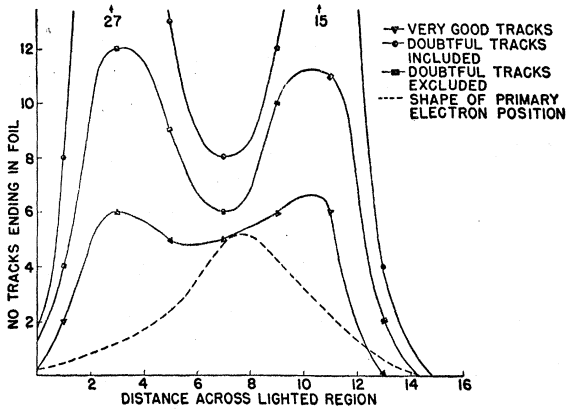

FIG. 3. Position distribution of tracks ending at a foil. They are classified according to their appearance. Shape of the incident electron distribution shows that many of the terminating tracks do not correspond to stopped electrons.

Some scattering of the incoming electrons occurred as they passed through the $\frac{1}{8}$-in. glass wall of the cloud chamber and through the successive lead foils. Consequently, a few tracks passed out of the lighted region and appeared near the foils only as faint tracks. The track counting was thus susceptible to error. For example, one could mistake a secondary electron knocked from a foil for a straggled electron following radiation. The policy established was to discard faint tracks consistently whether or not there appeared to be straggling. The lighted region in the chamber was 1.7 cm deep and fairly well-defined. Also the distribution of incident electrons across this region, as exemplified in Fig. 2, had few tracks near the boundaries. The possible error in observation, therefore, would be small.

A few tracks ended at the foils. One would expect an occasional electron to lose all or nearly all of its energy in a foil so that no straggled electron track could be seen. Also an electron may undergo elastic or inelastic scattering in a foil through an angle near 90 degrees and show very faintly or not at all. One wonders, therefore, how many terminated tracks to count as stopped electrons. A conscientious examination of these tracks was taken for part of the pictures. They were classified according to certainty, and their positions across the lighted region of the chamber were plotted. Figure 3 reveals that even among the best appearing events more terminated tracks appeared near the boundaries of the lighted region than in the middle. A comparison between the terminated track and incident electron track distributions indicates that scattering is responsible for the difference between them. The number of stopped electrons was assumed to correspond to the area under the

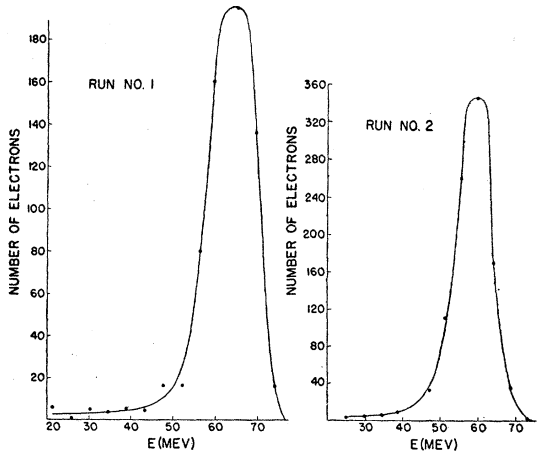

FIG. 4. Energy distribution of primary electrons. The mean energies of run 1 and run 2 are 62.5 and 57.8, respectively.

dashed curve. This number was then used as a contribution to the highest energy interval of the x-ray spectrum.

TREATMENT OF DATA

A. Calculation of the Cross Section

The experiment was performed with two energy distributions of the primary electrons. Figure 4 gives the two distributions with mean energies of 62.5 and 57.8 Mev, respectively. The corresponding widths at half-maximum intensity are roughly 13 and 10 Mev. The experimental results were determined separately for each distribution and then weighted results for the combined distributions were computed.

For convenience of presentation, the x-ray spectrum was calculated in terms of one maximum energy which was the arithmetic mean energy of the primary electrons. One minus the ratio of straggled electron to mean primary electron energy gave the fractional energy carried off by a quantum. A plot of the number of straggled electrons per Mev of energy *versus* the fractional energy loss so defined gave an experimental number spectrum of x-ray quanta. The corresponding theoretical spectrum was obtained by averaging over the primary energy distribution the cross section for production of each of a number of fixed, straggled electron energies. The slight distortion of this theoretical spectrum from that for monokinetic electrons of the mean energy is shown in Fig. 5.

The straggled electron energies were grouped in intervals of width equal to 0.05 of the mean energy. The atomic cross section for one interval in units of cm^2/Mev is

$$\phi_k = n/NWm, \qquad (1)$$

where n is the number of straggled electrons in the interval, N the number of primary or incident electrons, m the number of target atoms per cm^2 of foil, and W the width of the energy interval in Mev.

Of the number of observed straggled electrons, a few were classified as doubtful. Because of occasional close spacing of primary tracks, imperfect stereoscopic images, etc., they could not be classified with certainty as events in question. The doubtful events constituted 3 percent of the total number of events in all energy intervals from both five-mil and fifteen-mil foil data. Only half the doubtful events were retained. The number of doubtful tracks was quite small in all energy intervals except the one at the tip of the spectrum in which 10 of 84 tracks were in doubt. Retaining half the doubtful ones then left 79 events to be used.

B. Corrections

Two major corrections were applied to the data. One was a geometry correction. The other accounted for energy loss of electrons in the foils by multiple radiative and ionizing collisions.

The geometry correction resulted because many electrons, after traversing the lead foils, passed out of the lighted region in the cloud chamber without leaving sufficient track length for measurement of the energy loss. Because of the difficulty of making an accurate correction, several methods were used and compared.

The first method of correction retained tracks in a specified interval only with a chord length greater than a chosen minimum. Corresponding to a given minimum chord length was a maximum dip angle that the emergent track made with the horizontal plane, which was parallel to the boundaries of the lighted region. The magnitude of this angle depended upon the vertical position of the track at the foil in the lighted region. In general, the angle was double valued because of possible deflection up or down.

Corresponding to a minimum chord length K is a

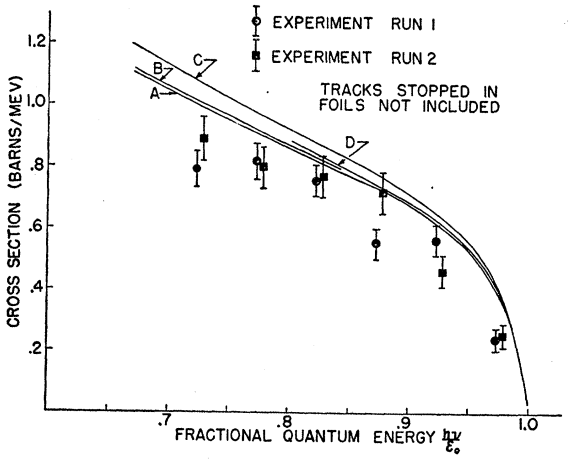

FIG. 5. Theoretical cross section and uncorrected results for two separate runs. $\mathcal{E}_0$ is the mean incident electron energy, and equals 62.5 Mev and 57.8 Mev, respectively, for runs 1 and 2. Correspondingly, curves B and C are the theory averaged over the two incident electron energy distributions above 38.9 Mev. Curve D is the average over energies above 27.5 Mev for run 1. Curve A is the theory for monoenergetic electrons of 62.5 Mev.

minimum ratio $\lambda_m = K/R$ with R the track radius. In determining the maximum dip angle α_M, a value of λ_m was chosen for each energy interval which was considerably greater than the smallest λ-value recorded. The particular value was such that it gave in the worst instance a probable error in measured radius corresponding to half the width of the energy interval. The radius of curvature of a track was measured by comparison of its arc with standard arcs scribed on a thin sheet of Lucite. The value of λ_m varied slowly with energy and had an approximate value of 0.29.

The use of λ_m together with the angular distribution of emergent tracks scattered out of the horizontal plane determined the fraction of events eliminated by the λ_m selection. The correct angular distribution of dip angles was inferred from the observed angular distributions and the assumption of angular symmetry about the incident direction. Figure 6 is an example of angular distributions that existed with respect to perpendicular planes. The ratio of the total area under the true dip angle curve to the area for angles less than α_M gave the correction factor to apply to the number of events in a given energy interval having $\lambda \geqslant \lambda_m$. Since not all stragglings occurred at the same vertical position in the lighted region, an integration was carried out over the incident electron position distribution.

A correction based on the angular symmetry method alone is independent of chord lengths, position distribution, and lighted region boundaries. It requires only that the angular distribution of straggled electrons be symmetrical in space about the incident electron direction. This should be true if there is no polarization of the incident electrons. The angular distribution should be circular on a polar coordinate graph, when no discrimination correction is necessary, and with adequate statistics. The observed angular distributions proved to be approximately elliptical.

Another method of correction consisted in retaining only those events for which the emergent tracks were deflected toward the central plane of the lighted region. Since straggled electrons should be deflected up and down in equal numbers, the same number should be

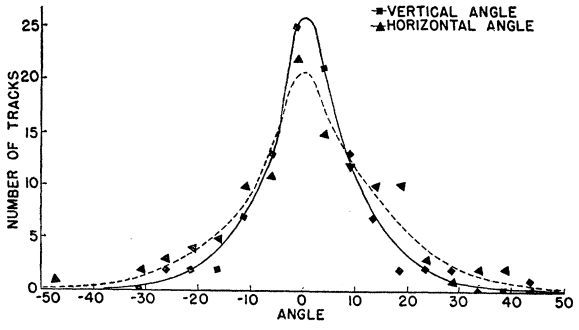

FIG. 6. Angular distribution of straggled electron tracks from 15-mil foil. Electrons have lost 0.875 times initial energy. The vertical and horizontal angles are angles made respectively with the horizontal plane and the vertical plane containing the primary electron direction at the foil.

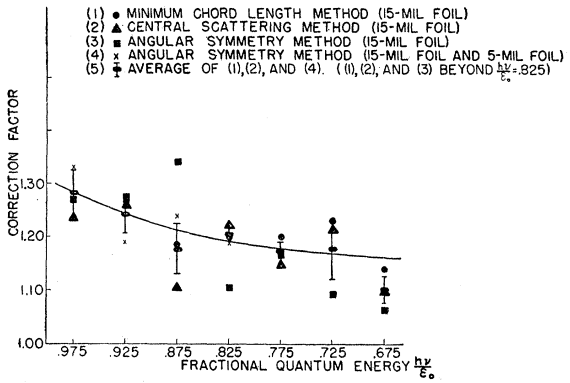

FIG. 7. Geometry correction to account for straggled electron tracks leaving the lighted region too abruptly for measurement.

deflected toward as away from the central plane of the lighted region. However, one can observe relatively more of the centrally deflected tracks for a given magnitude of deflection because of their greater lengths. In addition, the minimum chord length correction already described was applied to the centrally deflected tracks. This was smaller than that applied to all observed tracks. Retention of only the centrally deflected tracks appreciably reduces the statistics.

The three methods of correction described were used in correcting the one-foil data. Only the angular symmetry method was used for the five-foil data since not all the information necessary for the other methods was collected for these data. Figure 7 shows the correction for each method and the average correction to the total observed number of events as a function of energy. These corrections do not account for the number of electrons that may have stopped in the foils and which have already been discussed.

Because of the thickness of a foil, an electron may undergo successive radiation events while passing through it. Part of the energy loss will result also from ionizing collisions. Ionization after a large radiation loss may remove a straggled electron from one energy interval to another. This effect is increased by multiple scattering of the electron, particularly at low energy. To obtain an accurate bremsstrahlung cross section, the observed cross section must be corrected to that for an infinitely thin foil. The correction for multiple radiation loss is greater than that for ionization loss at all energies except for those near the tip of the x-ray spectrum. The net effect of the energy losses is to produce an increase in the observed cross section over the true cross section for most x-ray energies.

An electron of energy E_0 may lose energy by one or more successive radiative collisions down to an energy E' while passing through a foil. Unless the foil is very thick, the number of electrons emerging can be determined with sufficient accuracy by considering at most two successive radiation events. If η electrons of energy E_0 strike a foil of thickness t and n atoms per unit volume,

TABLE I. Energy loss correction. $\mathcal{E}_0=60.4$ Mev = primary electron energy. The calculations are first-order approximations for monokinetic electrons.

		435.9-mg/cm² foil			145.3-mg/cm² foils		
$\mathcal{E}$ (Mev)	$h\nu/\mathcal{E}_0$	Radiation correction	Ionization correction	Total correction	Radiation correction	Ionization correction	Total correction
1.51	0.975	−13.2%	−12.0%	−23.0%	−7.5%	−4.0%	−11.2%
4.53	0.925	−14.4	−1.8	−15.9	−8.2	≃0.6	−8.7
7.55	0.875	−11.7	−1.5	−13.0	−6.5	≃0.5	−6.9
10.57	0.825	−5.6	−1.7	−7.2	−3.2	≃0.6	−3.8
13.59	0.775	−2.6	−1.8	−4.3			
16.61	0.725	−1.8	−1.8	−3.6			
19.63	0.675	−4.7	−1.8	−6.4			

the number emerging with energy E' will be

$$N(E', t)\simeq\eta n^2\frac{t^2}{2}\int_{E'}^{E_0}\phi(E_0, E)\phi(E, E')dE + n\eta\left[t-\frac{nt^2}{2}\int_0^{E_0}\phi(E_0, E)dE\right]\phi(E_0, E'), \quad (2)$$

where $\phi(E, E')$ is the cross section per unit energy range. The two terms represent, respectively, the numbers of two collision events and one collision events. The two integrals diverge for the range of E near E_0; however, their difference remains finite there.

The number of electrons leaving energy E' while passing through the foil is approximately

$$\eta n^2\frac{t^2}{2}\phi(E_0, E')\int_0^{E'}\phi(E', E)dE. \quad (3)$$

The difference of (2) and (3) gives the number of straggled electrons emerging from the foil with energy E'. Division by ηnt gives the observed atomic cross section

$$\phi_k\simeq\phi_{k0}+\frac{nt}{2}\left\{\int_{E'}^{E_0}\phi(E_0, E)[\phi(E, E')-\phi_{k0}]dE - \phi_{k0}\int_0^{E'}\phi(E', E)dE-\phi_{k0}\int_0^{E'}\phi(E_0, E)dE\right\}, \quad (4)$$

where the cross section for an infinitely thin foil is $\phi_{k0}=\phi(E_0, E')$. The first two integrals diverge for the range of E near E'; however, their difference remains finite.

TABLE II. Uncorrected number of radiation events.

Foil thickness in mg/cm²	No. of foil traversals	No. of events for $h\nu/\mathcal{E}_0$ values 0.975	0.925	0.875	0.825	0.775	0.725	0.675
29.92	66016	5[a]	4	10	20			
145.9	97268	36[a]	66	79	88			
435.9	46628	43[a]	93	111	138	141	149	131[b]

[a] Does not include electrons stopped in a foil.
[b] Energy bin width is 0.79 times other bin widths, which are approximately 3 Mev wide.

From (4) the correction term to be applied to the observed cross section is proportional to the foil thickness to a first-order approximation. The correction was evaluated assuming the theoretical value for the cross section to be valid and using for E_0 the mean primary electron energy. Integration over the primary energy distribution would have appeared as a second-order effect and was not made. The first-order correction was less than 15 percent for all straggled electron energies for the thickest foil.

The straggled electrons emerge from a foil with a spread in angular distribution because of multiple scattering in the foil and because of a transverse component of momentum received in the bremsstrahlung process. The effective path length traversed by the straggled electrons after radiation has occurred is consequently increased. The increase is more pronounced for the lower energy electrons. This effect was included in an approximate manner by multiplying the correction term in Eq. (2) by $\sec\bar{\theta}$, where $\bar{\theta}$ was the observed mean angle that the emergent straggled electrons for each energy interval made with the incident direction.

There were five parallel foils across the cloud chamber for collection of the five-mil foil data. The effective value of t in Eq. (2) was increased a little over the five-mil thickness to account for some electrons undergoing two successive radiations in separate foils and not losing enough energy during the first collision for the resulting change in radius to be detected between foils. For this calculation the maximum energy which could be detected was taken as 30 Mev. The effective value of t was not critically dependent upon this choice.

Energy loss of the straggled electrons by ionization in the foils of thickness t was calculated by assuming the effective path length to be $\frac{1}{2}t\sec\bar{\theta}$ and by using Bloch's well-known formula for collision loss. The shape of the x-ray spectrum and the slow variation in amount of ionization with energy result in more straggled electrons entering than leaving a given energy interval. For the lowest electron energy interval there can be a flux of electrons only into the interval.

The results of the two types of energy loss corrections are tabulated in Table I. All energies listed are for the mid-points of energy intervals. The correction to the observed cross section is negative for both energy loss effects.

RESULTS AND CONCLUSIONS

Table II and Figs. 8–10 contain the most significant data and results for the bremsstrahlung cross section. The cross sections are in units of barns (10^{-24} cm^2) per nucleus per Mev of straggled electron or x-ray energy. $h\nu/\mathcal{E}_0$ is the ratio of radiation quantum energy to the mean kinetic energy of the primary electrons. The point spreads on the graphs are probable errors resulting from the statistics and the uncertainties in the geometry corrections. A substantial part of the uncertainty in the five-mil foil results arose through the geometry corrections based on only the angular symmetry method.

Because of the poor statistics, no attempt was made to correct the one-mil foil results. The uncorrected total cross section for the top four energy intervals of the spectrum is 6.8 barns compared with the theoretical value of 7.78 barns. Both the negative energy loss correction and the positive geometry correction should

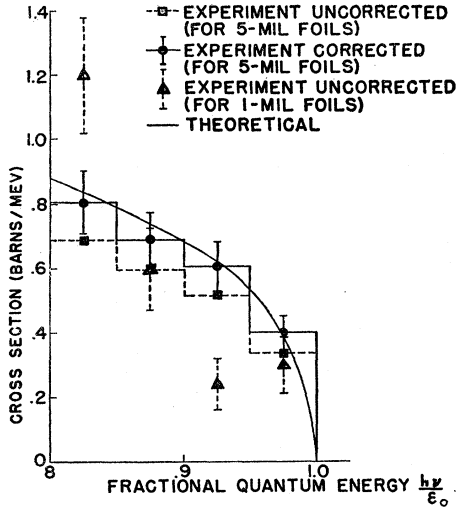

FIG. 8. Results from 5-mil and 1-mil foils.

be smaller than for the five-mil and fifteen-mil foil results because of the thinner foils and less multiple scattering.

The total cross section for the five-mil foil data for the top of the x-ray spectrum from 50 to 62.8 Mev is 7.8 $\pm$0.5 barns compared with 8.07 barns from theory. The combination of fifteen-mil and five-mil foil results represents better statistics and gives for the top 12.28-Mev energy range of the spectrum a total cross section of 7.5$\pm$0.3 barns compared with 8.00 barns from theory. The total cross section for the top 20.48 Mev of the spectrum determined from the fifteen-mil foil data is 15.2$\pm$0.6 barns compared with 16.52 barns from theory or 8 percent lower. The theoretical values here do not include the contribution from bremsstrahlung production in the field of orbital electrons. This correction would be no more than 1 percent.

Within experimental uncertainties, the top 30 percent of the x-ray spectrum agrees with the Bethe-Heitler

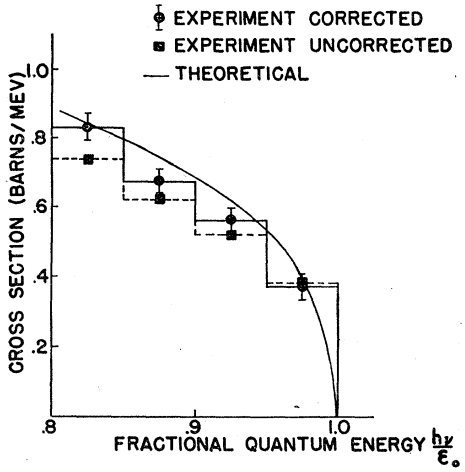

FIG. 9. Combined results from 5-mil and 15-mil foils.

theory in shape. However, the magnitude of the bremsstrahlung cross section appears a few percent lower than theory.

The pair production process is much like the reverse of bremsstrahlung production. Many x-ray absorption and pair production experiments[6,23–26] have indicated that the cross section for pair production in heavy elements relative to that in light elements is lower than that given by the Bethe-Heitler theory using the Born approximation. For example, Emigh[26] gives a pair cross section for gold relative to aluminum 7.9$\pm$1.5 percent lower than theory for x-rays in the range 50 to 300 Mev from a 300-Mev betatron.

The present experiment was in part an exploratory study of a method for obtaining an absolute bremsstrahlung cross section and spectral shape. There is room for improvement of the statistics and of the experimental techniques to reduce the uncertainties. Among the most

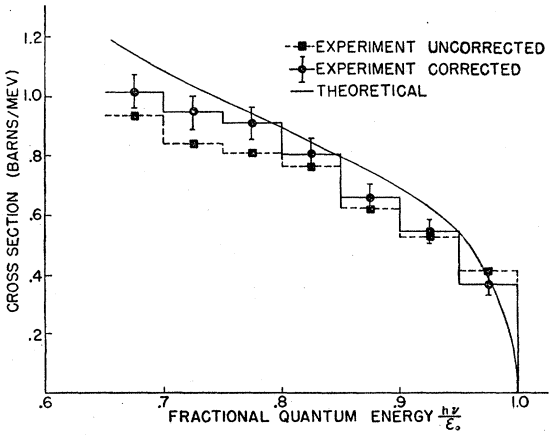

FIG. 10. Results from 15-mil foils.

[23] R. L. Walker, Phys. Rev. **76**, 527 (1949).
[24] J. L. Lawson, Phys. Rev. **75**, 433 (1949).
[25] Dewire, Ashkin, and Beach, Phys. Rev. **83**, 505 (1951).
[26] C. R. Emigh, Phys. Rev. **86**, 1028 (1952).

important improvements in further work of this type would be the use of a nearly monokinetic electron beam obtained directly from the accelerator or with the aid of a larger analyzer magnet. The electron beam should be well centered in a deeply lighted region with little vertical spread. A long entrance window would minimize scattering of the primary electrons. The chamber should be larger and have a stronger magnetic field applied than in the present experiment if more of the spectrum were to be examined at the same primary energy. In this connection, the problem caused by a wide angular distribution of straggled electrons would become less acute for a given point on the spectrum. The use of higher primary electron energies would permit examination of the high energy end of the spectrum in more detail.

The author wishes to acknowledge with gratitude the advice, suggestions, and encouragement of Professor Donald W. Kerst, who directed this work. He also wishes to express his appreciation to Dr. H. W. Koch who designed much of the cloud-chamber equipment. This experiment was in part a culmination of early interest stimulated in radiation straggling by Dr. L. S. Skaggs. The collection and analysis of data were carried forward with the able assistance of P. C. Fisher, J. W. Henderson, G. Modesitt, and J. H. Malmberg.

PHYSICAL REVIEW VOLUME 89, NUMBER 1 JANUARY 1, 1953

Effect of Equatorial Ring Current on Cosmic-Ray Intensity*

S. B. TREIMAN†
Institute for Nuclear Studies, University of Chicago, Chicago, Illinois
(Received August 25, 1952)

The equatorial ring current postulated by Chapman and Ferraro to explain the main phase of terrestrial magnetic storms is analyzed with respect to its effect on the intensity of the cosmic radiation. For mathematical convenience, the ring current is replaced by a current sheet located on the surface of a sphere concentric with the earth, in accordance with a suggestion due to Chapman. A simple expression is then obtained relating the variations in magnetic field at the equator with the corresponding variations to be expected in the intensity of cosmic radiation measured by an arbitrary detector located at any latitude and atmospheric depth.

I. INTRODUCTION

IT is well known that terrestrial magnetic storms are due, in part, to current systems located above the surface of the earth. In particular, Chapman and Ferraro[1] have postulated the existence of a westward-flowing ring of current which encircles the earth in the magnetic equatorial plane and which has a radius several times that of the earth. It is supposed that the current decays slowly during the periods between storms but that it is enhanced from time to time by corpuscular beams from the sun, the resulting current variations giving rise to the magnetic disturbances observed on the earth during the main phase of magnetic storms.

Now one can, of course, imagine an infinite number of current systems which could produce the magnetic disturbances observed on the earth's surface. In order to provide an independent test of the ring current theory, therefore, Chapman[2] has suggested that it would be profitable to study the effect of such a current system on the cosmic radiation.

In the following, an attempt is made to determine the variations in cosmic-ray intensity that would be expected to accompany variations in the intensity of the postulated ring current. The calculations are carried out in the approximation corresponding to the Stoermer theory of allowed cones in the field of a simple dipole, i.e., the effect of the ring current on the Stoermer cones is calculated and the assumption is then made that all directions within the modified cones are "allowed." Considerations of the earth's shadow and of the finer details of the Lemaitre-Vallarta theory are neglected. Although we speak here of a "ring" current, the calculations are actually carried out for a simpler current system which approximates the effect of a ring current.

II. DETERMINATION OF THE ALLOWED CONES

We consider the motion of a particle of charge e in the combined magnetic fields of the earth's dipole and of a ring current encircling the earth in the magnetic equatorial plane. The coordinate system is shown in Fig. 1. The positive z axis points toward the earth's magnetic north. The earth's dipole M_e is located at the origin and is directed along the negative z axis. The earth's radius is designated by ρ, and the radius of the ring is taken to be $a\rho$; θ is the angle between the velocity vector of the particle and the meridian plane, where θ is positive if the particle crosses the meridian plane from east to west.

* Assisted by the Air Research and Development Command, USAF.
† Now at Palmer Physical Laboratory, Princeton University, Princeton, New Jersey.
[1] S. Chapman and V. Ferraro, Terr. Mag. Atmos. Elec. **45**, 245 (1940), and references therein.
[2] S. Chapman, Nature (London) **140**, 423 (1937).